Effect of the niobium state on the properties of NbSiBEA as bifunctional catalysts for gas- and liquid-phase tandem processes

Pavlo I. Kyriienko, Olga V. Larina, Nataliia O. Popovych, Sergiy O. Soloviev,
Yannick Millot, Stanislaw Dzwigaj

HAL Id: hal-01346172

https://hal.sorbonne-universite.fr/hal-01346172v1

Submitted on 18 Jul 2016

Effect of the niobium state on the properties of NbSiBEA as bifunctional catalysts for gas- and liquid-phase tandem processes

Pavlo I. Kyriienko[a],*, Olga V. Larina[a], Nataliia O. Popovych[a], Sergiy O. Soloviev[a], Yannick Millot[b], Stanislaw Dzwigaj[b],*

[a] L.V.Pisarzhevsky Institute of Physical Chemistry of the NAS of Ukraine

31 Prosp. Nauky, 03028 Kyiv, Ukraine

[b] Sorbonne Universités, UPMC Univ Paris 06, CNRS, UMR 7197, Laboratoire de Réactivité de Surface, F-75005, Paris, France

* Corresponding authors:

Pavlo I. Kyriienko, e-mail address: pavlo_kyriienko@ukr.net

Stanislaw Dzwigaj, e-mail address: stanislaw.dzwigaj@upmc.fr

Graphical Abstract

Active sites of NbSiBEA zeolite in tandem processes

Highlights

Mononuclear and polynuclear Nb(V) were identified in NbSiBEA zeolites.

The state of niobium in NbSiBEA zeolite determined its catalytic properties.

Higher TOF and TON values were achieved on NbSiBEA with framework mononuclear Nb(V).

Bifunctional catalyst for tandem processes was designed using two-step postsynthesis method.

Abstract

NbSiBEA zeolites contained isolated framework mononuclear Nb(V) ($Nb_{0.7}SiBEA$) and a mixture of framework mononuclear and extra-framework polynuclear Nb(V) ($Nb_{2.0}SiBEA$) were prepared by two-step postsynthesis method as evidenced by XRD, NMR, DR UV-vis and FTIR. DR UV-vis showed that two types of framework mononuclear Nb(V) are present in $Nb_{0.7}SiBEA$, while $Nb_{2.0}SiBEA$ mainly contained isolated mononuclear Nb(V) in the framework of zeolite and polynuclear Nb(V) in the extra-framework position. FTIR with pyridine and 2,6-di-*tert*-butylpyridine as probe molecules showed that major amount Lewis and weak Brønsted acidic sites are formed by incorporation of niobium in the framework of zeolites as mononuclear Nb(V). The catalytic properties of Nb-containing zeolites were investigated in tandem processes of ethanol conversion into 1,3-butadiene (gas-phase) and synthesis of unsymmetrical ethers from aromatic aldehyde and aliphatic alcohol (liquid-phase). It has been found that $Nb_{0.7}SiBEA$ catalyst, containing only isolated framework mononuclear Nb(V) is more active than $Nb_{2.0}SiBEA$ in the conversion of ethanol and ethanol/acetaldehyde mixture into 1,3-butadiene, MPV reduction of crotonaldehyde with ethanol and etherification of 4-methoxybenzyl alcohol with 2-butanol. The higher specific activity (turnover number/frequency) of $Nb_{0.7}SiBEA$ than $Nb_{2.0}SiBEA$ catalyst has been revealed for gas- and liquid-phase tandem processes.

1. Introduction

Niobium-containing materials are widely studied as solid catalysts for heterogeneous processes including sustainable organic synthesis [1]. Nb_2O_5/SiO_2 catalysts are active in sugar dehydration [2–5], methanol oxidation [6], glycerol dehydration to acrolein [7] and oxidation reactions with aqueous H_2O_2 [8–11]. Catalysts based on niobium oxides were also used in the process of ethanol (EtOH) conversion to 1,3-butadiene (BD) [12,13].

Coordination state of niobium in a carrier matrix significantly influences the activity of niobium-containing sites in a catalyst. Guidotti with co-workers [8] reported that Nb/SiO_2 catalysts, prepared by a co-precipitation method, have higher activity and stability in alkenes epoxidation in the presence of aqueous hydrogen peroxide due to the conservation of coordination state and uniform distribution of Nb on the carrier surface in contrast to Nb/SiO_2 prepared by deposition. NbBEA zeolites, obtained by direct hydrothermal synthesis, catalyze Meerwein-Ponndorf-Verley (MPV) reduction and etherification processes more effectively than samples prepared by impregnation [14]. The similar effect was observed for Zr-containing systems in EtOH conversion to BD [15] i.e. greater specific catalytic activity of ZrBEA in comparison with Zr/MCM-41 and ZrO_2/SiO_2 was caused by higher content of isolated Zr(IV) sites in the ZrBEA catalyst.

We have recently shown [16] that two-step postsynthesis method of tantalum incorporation in BEA zeolite framework as isolated mononuclear Ta(V) allows preparing highly selective tantalum-silicate catalysts for the conversion of EtOH and acetaldehyde (AA) mixture into BD. A clear distinction between postsynthesized and hydrothermally synthesized SnBEA zeolites was showed in Baeyer-Villiger and MPV reactions [17,18]. Catalytic activity of dealuminated Sn-containing BEA zeolite is supposed to be associated with the structural difference of Sn-containing active sites, especially with the presence of frustrated Lewis acid-base pairs with outersphere coordination of SiO^-. Obviously, incorporation of metals in a

framework of dealuminated BEA zeolite is a more convenient way to form isolated metal species in the silicate matrix.

This paper is aimed to study the effect of the niobium state present in BEA zeolite matrix on the activity and selectivity of NbSiBEA catalysts in so-called tandem processes, requiring different types of active sites (redox and/or acid-base). In particular, the Nb-containing catalysts were tested in gas- and liquid-phase processes: (1) EtOH conversion to BD, and (2) direct synthesis of unsymmetrical ethers from aromatic aldehyde and aliphatic alcohol (4-methoxybenzaldehyde and 2-butanol).

2. Experimental

2.1. Catalysts preparation

A tetraethylammonium BEA was placed in a aqueous solution of 13 mol·L^{-1} HNO$_3$ and lasted at 353 K during 4 h to obtain a dealuminated organic-free BEA, as previously described [19,20]. The obtained SiBEA (Si/Al = 1300) with vacant T-atom sites was recovered by centrifugation, washed with distilled water and dried in air at 353 K during 24 h.

In order to introduce niobium ions into framework of BEA zeolite, two portion of 2 g of SiBEA were stirred for 3 h at 353 K in 100 mL of isopropanol (dry) solutions containing 1.5×10^{-3} and 4.4×10^{-3} mol·L^{-1} Nb(OC$_2$H$_5$)$_5$ (Alfa Aesar, 99.999 %), respectively. Then, two suspensions at pH = 5.6 and 2.5, respectively, were stirred in air at 353 K for 1 h to evaporate the solvent. The resulting samples were washed in distilled water (three times), dried (in air at 353 K for 24 h) and calcined (in flowing air at 723 K for 3 h). The obtained samples containing 0.7 and 2.0 wt % of Nb were labeled Nb$_{0.7}$SiBEA and Nb$_{2.0}$SiBEA, respectively.

2.2. Catalysts characterization

The chemical analysis of zeolites was performed with ICP atom emission spectroscopy at the CNRS Centre of Chemical Analysis (Vernaison, France).

Textural properties of studied samples were determined by low-temperature (77 K) N_2 sorption on an Autosorb-1 (Quantachrome, USA). The zeolites, before analysis, were treated under vacuum at 383 K for 18 h. The specific surface area was calculated from the BET method and the micropore volume was determined using Vt-plot method.

X-ray diffraction (XRD) patterns of the powder samples were recorded using D8 Advance (Bruker AXS GmbH, Germany) diffractometer with monochromatized Cu-Kα radiation (nickel filter, λ = 0.15418 nm). The d_{302} spacing was calculated using equation:

$$n\lambda = 2d \cdot \sin\theta$$

where n is an integer (n = 1), λ is the wavelength of incident wave, d is the spacing between the planes in the atomic lattice, and θ is an angle between the incident ray and the scattering planes.

NMR spectra were registered using Avance 400 spectrometer (Bruker, Germany). ^{29}Si MAS NMR spectra were recorded at 79.5 MHz using 7 mm (external diameter) zirconia rotors, with CP (^1H - ^{29}Si CP-MAS NMR) and without (^{29}Si MAS NMR). Chemical shifts of silicon were measured relative to tetramethylsilane (TMS). ^{29}Si MAS NMR spectra were obtained with rotors spinning speed of 4 kHz, excitation pulse duration of 2.5 μs and recycle delay of 10 s. Polydimethylsilane (PDMS) was used for setting the Hartmann-Hahn condition. The proton π/2 pulse duration, the contact time and recycle delay were 6.8 μs, 5 ms and 5 s, respectively. ^1H MAS NMR spectra were recorded using 4 mm zirconia rotors with a 90° pulse duration of 3 μs and a recycle delay of 6 s.

Diffuse reflectance (DR) UV–vis spectra were recorded at ambient atmosphere with polytetrafluoroethylene as reference using Cary 5000 spectrometer (Varian, USA) equipped with a double integrator.

Fourier Transform Infrared Spectroscopy (FTIR) spectra were recorded at a spectral resolution of 1 cm^{-1} on KBr pellets using a Spectrum One FTIR spectrometer (Perkin Elmer, USA).

Transmission FTIR spectra of self-supported wafers were recorded using a Vertex 70 spectrometer (Bruker, Germany) accumulating 128 scans at a resolution of 2 cm^{-1}. The wafers were activated by calcination at 723 K for 2 h in flowing 2.5% O_2 in Ar and then outgassed at 573 K (10^{-3} Pa) for 1 h before each measurement.

Analysis of acidic properties of the zeolites was performed by adsorption of pyridine and 2,6-di-tert-butylpyridine (DTBP) followed by infrared spectroscopy. Before analysis, the samples were pressed at ~ 2 ton·cm^{-2} into thin wafers of ca. 12 mg·cm^{-2} and placed inside the IR cell. FTIR spectra with pyridine or DTBP were recorded on a Spectrum One FTIR spectrometer (Perkin Elmer, USA) accumulating 48 scans at a spectral resolution of 1 cm^{-1}. The cell was connected to a vacuum-adsorption apparatus allowing a residual pressure below 10^{-3} Pa. The spectra were recorded under ambient conditions after pyridine desorption at 423, 523, 573 and 623 K and after DTBP desorption at 423 K. Before pyridine or DTBP adsorption, the samples were outguessed (10^{-3} Pa) at 673 K for 1 h. All measured spectra were recalculated to a "normalized" wafer weight.

2.3. Catalytic activity measurement

2.3.1. Gas-phase process

Catalytic activity tests were carried out at 1 bar in a fixed-bed flow (quartz) reactor with inner diameter of 4 mm. Samples with grains of 0.25–0.5 mm (0.25 g,) were used. Before reaction the samples were treated at 673 K under flowing argon for 1 h. EtOH or the mixtures of EtOH/AA and EtOH/crotonaldehyde were fed into the catalytic reactor (weight hourly space velocity (WHSV) = 0.8 $g_{reagents}·g_{cat}^{-1}·h^{-1}$, with Ar as a carrier gas and a flow rate of 15 mL/min). The reagents and obtained products were analyzed chromatographically (KristalLyuks 4000M, MetaChrom, Russia). To identify CO, CO_2 a thermal conductivity detector and a packed column (10% $NiSO_4$ on coal, 3 m × 3 mm) were used, for organic compounds –a flame ionization detector and a capillary column (HP-FFAP, 50 m × 0.32 mm).

Total conversion (*TC*) of the reagents (EtOH, EtOH/AA and EtOH/crotonaldehyde mixtures), selectivity to products (*S_j*) and BD yield (*Y_BD*) were calculated by the following formulas:

$$TC = \frac{\sum n_i^0 - \sum n_i}{\sum n_i^0} \cdot 100, \%$$

$$S_j = \frac{n_j}{\sum n_i^0 - \sum n_i} \cdot 100, \%$$

$$Y_{BD} = TC \cdot S_{BD} / 100, \%$$

where n_i^0 is the initial amount of C moles of the reagents, n_i and n_j are the amount of C moles of the unreacted reagents i and product j in the stream of the reaction products.

Turnover frequency (*TOF*) was obtained by dividing the number of moles of reacted reagent(s) or obtained product(s) with number of moles of Nb per one hour.

2.3.2 Liquid-phase process

Zeolite catalyst (100 mg) after activation (773 K, 2 h) was added to the stock solution of 4-methoxybenzaldehyde (**1**) (1.25 mmol) in 2-butanol (4 g). The reaction mixture was heated to 353 K with vigorous stirring. At various time intervals, aliquots were taken from the reaction mixture and analyzed after separation of the catalyst by centrifugation. The progress of the reaction was analyzed by a gas chromatograph (KristalLyuks 4000M, MetaChrom, Russia) equipped with an FID detector and a capillary column (HP-FFAP) using mesitylene as an internal standard for quantification. The reactants and products were identified on the basis of coincidence of retention times with those of extra pure standards.

Catalytic activity was characterized by the conversion (*C*) of aldehyde **1** and selectivities of products (*S_k*).

$$C = \frac{n_{Ald.1}^0 - n_{Ald.1}}{n_{Ald.1}^0} \cdot 100, \%$$

$$S_k = \frac{n_k}{n_{Ald.1}^0 - n_{Ald.1}} \cdot 100, \%$$

where $n^0_{Ald.1}$ is the initial amount of C moles of aldehyde **1**, $n_{Ald.1}$ and n_k are the amount of C moles of aldehyde **1** and product k in the reaction products.

Turnover number (*TON*) was calculated as number of moles of reacted aldehyde **1** (after 10 h) divided by number of moles of Nb.

For the etherification reaction of 4-methoxybenzyl alcohol (**2**) with 2-butanol, the stock solution, containing alcohol **2** (2.5 mmol) in 2-butanol (4 g) was used. The progress of the reaction was analyzed as described hereinabove.

3. Results and discussion

3.1. Prove for the incorporation of Nb in BEA zeolite

The samples prepared by postsynthesis method, hereafter referred to as Nb$_{0.7}$SiBEA and Nb$_{2.0}$SiBEA, are white and contain 0.7 and 2.0 Nb wt %.

The textural properties of HAlBEA, SiBEA, Nb$_{0.7}$SiBEA and Nb$_{2.0}$SiBEA were studied by means of low-temperature nitrogen sorption. Fig. 1 exhibits nitrogen sorption isotherms of all samples. All of them are type I according to IUPAC. The values of BET specific surface area and micropore volumes of HAlBEA, SiBEA, Nb$_{0.7}$SiBEA and Nb$_{2.0}$SiBEA were in the ranges of 460−491 m^2 g^{-1} and 0.19–0.21 cm^3 g^{-1}, respectively (Table 1) characteristics of BEA zeolite.

XRD patterns of SiBEA, Nb$_{0.7}$SiBEA and Nb$_{2.0}$SiBEA are typical for BEA zeolite (Fig. 2). Dealumination of BEA zeolite with HNO$_3$ and following incorporation of niobium ions in the framework of SiBEA zeolite as mononuclear Nb(V) does not affect structure crystallinity, in line with earlier reports [21,22]. The shift of diffraction peak about 22.6º as a result of removal of Al atoms from zeolite framework and incorporation of metal ions is used as prove for zeolite matrix contraction/expansion [19,20,23]. The significant decrease of the d$_{302}$ spacing from 3.943 Å (HAlBEA; 2θ = 22.55°) to 3.920 Å (SiBEA; 2θ = 22.67°) upon dealumination suggest contraction of the BEA matrix. A strong increase of d$_{302}$ spacing from 3.920 Å (SiBEA; 2θ = 22.67°) to 3.957 (Nb$_{0.7}$SiBEA; 2θ = 22.44º) and 3.946 Å (Nb$_{2.0}$SiBEA; 2θ = 22.50º) observed

after incorporation of Nb into SiBEA points out its expansion due to longer Nb–O bond length (1.89 for tetracoordinated Nb(V) in BEA zeolite [14]) as compared with Si–O (typically 1.60–1.65 Å in zeolites [24]). The lower increase of d_{302} value appeared for $Nb_{2.0}$SiBEA than for $Nb_{0.7}$SiBEA and $Nb_{1.0}$SiBEA, $Nb_{1.5}$SiBEA, $Nb_{1.6}$SiBEA [21,22] with only framework mononuclear Nb(V) suggests that for former zeolite only a part of niobium was incorporated in the zeolite framework.

The ^{29}Si MAS NMR spectrum of SiBEA (Fig. 3) contains signals at -102.3, -111.0 and -114.3 ppm. The peaks at -111.0 and -114.3 ppm are caused by framework Si atoms in $Si(OSi)_4$ environment, located at different crystallographic sites [25]. The peak at -102.3 ppm is attributed to Si atoms in $Si(OH)(OSi)_3$ environment. It is confirmed by a significant increase of intensity of the peak at -102.3 ppm when $^1H – ^{29}Si$ CP-MAS NMR technique is applied (Fig. 4), since the signal of ^{29}Si nuclei close to protons is preferentially enhanced.

After incorporation of niobium ions in SiBEA, the intensity of the peak at about -102 ppm is noticeably decreased for $Nb_{0.7}$SiBEA and $Nb_{2.0}$SiBEA (Fig. 3). It confirms the reaction between niobium ethoxide ($Nb(OC_2H_5)_5$) precursor and silanol groups of vacant T-atoms. However, the absence of further decrease of the peak at -102.2 ppm after introduction of more amount of niobium ($Nb_{2.0}$SiBEA) suggests that major part of niobium is not incorporated in framework of $Nb_{2.0}$SiBEA. It seems that these niobium ions are introduced in extra-framework position of BEA zeolite as polynuclear Nb(V). In contrast, for $Nb_{0.7}$SiBEA the peak at -102.4 ppm prove that almost all niobium is incorporated as isolated mononuclear Nb(V).

The change of the $Si(OSi)_4$ environment takes place upon incorporation of Nb ions in SiBEA as deduced from the appearance of the well distinguished ^{29}Si MAS NMR peaks at -114.0 and -114.1 ppm for $Nb_{0.7}$SiBEA and $Nb_{2.0}$SiBEA, respectively (Fig. 3). In contrast, for SiBEA only shoulder is present at around -114.3. It suggests that the incorporation of Nb in SiBEA modify the silicon environment.

Concerning ^{1}H MAS NMR spectra (Fig. 5), two main peaks are observed at 1.4 and 5.4 ppm for SiBEA, indicating the presence of protons of isolated (and/or terminal) SiO-H and hydrogen bonded silanol groups at vacant T-atom sites, respectively [26,27]. A small peak at 3.3 ppm is due to protons of H-bonded silanol groups present in a second kind of crystallographic sites. This shift is comparable with that observed at 3.20 ppm for H-bonded silanol groups in silica and silicalite [28,29]. The disappearance of the peak at 5.4 ppm after incorporation of Nb in SiBEA (Fig. 5) proves the reaction of niobium ethoxide precursor with both H-bonded silanol groups. The ^{1}H MAS NMR spectra of $Nb_{0.7}SiBEA$ and $Nb_{2.0}SiBEA$ allow distinguishing the peak with high intensity at around 3.8–4.1 ppm and two other peaks with low intensity at 2.0 and 1.2 ppm. The peaks with low intensity are probably due to protons of isolated and terminal silanol, respectively [30], still present in $Nb_{0.7}SiBEA$ and $Nb_{2.0}SiBEA$ after incorporation of Nb into the vacant T-atom sites of SiBEA.

The DR UV–vis spectrum of $Nb_{0.7}SiBEA$ demonstrates the presence of two absorption bands at 220 and 234 nm (Fig. 6) corresponding to different mononuclear Nb(V) present in the framework of BEA zeolite and are assigned to oxygen-tetrahedral Nb(V) ligand-to-metal charge transfer transitions [21,22,31,32]. The absence of bands at around 330–450 nm assigned to niobia-like phases [31,33] indicates that these form of Nb species are not present in $Nb_{0.7}SiBEA$.

In the DR UV–vis spectrum of $Nb_{2.0}SiBEA$ the three bands at 228, 248 and 370 nm (Fig. 6) appear corresponding to Nb(V) framework mononuclear Nb(V) (band at 228 nm), extra-framework polynuclear Nb(V) (248 nm) and niobium oxides (370 nm) [6]. Lower intensity of the band at 228 nm on $Nb_{2.0}SiBEA$ than the bands at 220 and 234 nm on $Nb_{0.7}SiBEA$ spectrum reveals lower content of mononuclear Nb(V) in $Nb_{2.0}SiBEA$ than in $Nb_{0.7}SiBEA$. The absence of (d–d) transitions for both $Nb_{2.0}SiBEA$ and $Nb_{0.7}SiBEA$ in the range of 600–800 nm suggests that Nb(IV) species are not present.

After treatment of TEABEA zeolite with acid nitric the bands attributed to the OH stretching modes of AlO-H groups (3782 and 3665 cm^{-1}) and Al-O(H)-Si groups (3608 cm^{-1})

[19,34] are not observed in the spectrum of SiBEA (Fig. 7), proving the full removal of aluminium. The occurring of narrow bands at 3736 and 3705 cm^{-1} and a broad band at 3515 cm^{-1} related to isolated SiO-H groups and H-bonded SiO-H groups, respectively, proves the formation of vacant T-atom sites in SiBEA, as reported previously [34]. The incorporation of niobium in the zeolite induces a reduction of intensity of all these bands, suggesting the reaction of SiO-H groups, with the niobium precursor. For $Nb_{0.7}$SiBEA and $Nb_{2.0}$SiBEA a band at 3745 cm^{-1} appears in the spectra, related to Nb(V)O-H.

The niobium incorporation in SiBEA modifies the Si environment as shown by changes of the stretching vibration of Si–O [22]. The band at 955 cm^{-1} observed in FTIR spectrum of SiBEA reveals the presence of Si-O group in vacant T-atom sites, as reported previously [20]. The incorporation of niobium into these sites modifies the Si–O stretching vibration that appears at higher wavenumber (960 cm^{-1}) on both $Nb_{0.7}$SiBEA and $Nb_{2.0}$SiBEA FTIR spectra than on SiBEA spectrum (955 cm^{-1}) (Fig. 8). The modifications of the band at 1223–1238 cm^{-1} characteristic of BEA zeolite and associated with the specific arrangement of tetrahedral Si(IV) sites are due to the increase of the unit cell parameter upon incorporation of niobium into the framework (XRD results, Fig. 2).

FTIR spectra of pyridine adsorbed on $Nb_{0.7}$SiBEA and $Nb_{2.0}$SiBEA are seen in Fig. 8. The bands at 1445, 1578 and 1596 cm^{-1} correspond to weakly bonded pyridine [35], as proved by their disappearance after desorption of pyridine at 523 K. In contrast, the bands appeared at 1450, 1600 and 1611 cm^{-1} correspond to pyridine coordinatively bonded to Lewis acidic sites (LAS) (Nb(V) species) [36]). The intensity of absorption bands at 1611 and 1600 cm^{-1} for $Nb_{2.0}$SiBEA is comparable to $Nb_{0.7}$SiBEA, which contains almost three times less niobium. It suggests that major amount of LAS are formed by niobium introduced in the framework of SiBEA as mononuclear Nb(V). The intensity of these bands for SiBEA is much lower than for $Nb_{0.7}$SiBEA and $Nb_{2.0}$SiBEA, as reported earlier [21,37] and proves that they are related to pyridine adsorbed on niobium.

The Lewis acidic sites (LAS) concentrations has been calculated from intensity of the band at 1450 cm^{-1} corresponding to pyridine coordinately bonded to Lewis acidic sites observed in FTIR spectra after adsorption of pyridine at room temperature and then desorption at different temperatures 423, 523, 573 and 623 K. The results for Nb$_{0.7}$SiBEA and Nb$_{2.0}$SiBEA are shown in Table 2. The similar concentration values obtained for Nb$_{0.7}$SiBEA and Nb$_{2.0}$SiBEA after desorption of pyridine at different temperatures indicate that LAS are mainly formed upon incorporation of niobium in the framework of SiBEA zeolite.

Brønsted acidic sites (BAS) were not identified in both Nb$_{0.7}$SiBEA and Nb$_{2.0}$SiBEA samples (the band of pyridinium cations at 1550 cm^{-1} on FTIR spectra is absent, Fig. 9 A and B).

DTBP as stronger base than pyridine has been used to establish presence of weak BAS preferentially on external surface. FTIR spectra of DTBP adsorbed on Nb$_{0.7}$SiBEA and Nb$_{2.0}$SiBEA are presented in Fig. 10. According to previous works [38,39], the bands at 1615 and 1532 cm^{-1} are assigned to the protonated DTBP adsorbed on BAS. The intensity of these bands is slightly higher for Nb$_{0.7}$SiBEA than for Nb$_{2.0}$SiBEA, indicating the higher amount of weak BAS in former than in latter zeolite.

Thus, incorporation of niobium into the framework of SiBEA as mononuclear Nb(V) is proved by XRD, DR UV-vis, NMR and FTIR. DR UV-vis study shows that two types of framework mononuclear Nb(V) are present in Nb$_{0.7}$SiBEA, while Nb$_{2.0}$SiBEA contains both framework mononuclear Nb(V) and extra-framework polynuclear Nb(V). The presence of Lewis acidic sites, formed by framework mononuclear Nb(V), and weak Brønsted acidic sites was identified by FTIR using pyridine and DTBP as probe molecules.

3.2. Catalytic properties of NbSiBEA zeolites in tandem processes

3.2.1. Gas-phase process: conversion of EtOH into BD

Scheme 1 shows consecutive steps of gas-phase process of EtOH conversion to BD, such as AA formation from EtOH, aldol condensation of AA to acetaldol, dehydration of acetaldol to

crotonaldehyde, Meerwein–Ponndorf–Verley reduction of crotonaldehyde with EtOH to crotyl alcohol and AA, and dehydration of crotyl alcohol to BD [40,41]. Scheme 1 also shows the main side process, which is EtOH dehydration to diethyl ether (DEE) and then to ethylene. Consequently, bifunctional catalyst capable of catalyzing both hydrogen transfer (redox process), and aldol condensation and dehydration, is necessary for selective BD synthesis from ethanol [42–45].

EtOH conversion. The catalytic performance of NbSiBEA zeolites has been shown in Table 3. The main products of EtOH conversion are BD, AA, ethylene and DEE. Small quantity of crotonaldehyde was identified. In the presence of $Nb_{0.7}$SiBEA almost two times higher yield of BD is achieved than on $Nb_{2.0}$SiBEA due to greater EtOH conversion and selectivity to BD. Another difference between two catalysts could be seen from the selectivities toward formation of the products of EtOH dehydrogenation (AA) and dehydration (ethylene + DEE). Higher residual amount of AA observed for $Nb_{2.0}$SiBEA catalyst could indicate the lower quantity of sites of aldol condensation on its surface. High selectivity to ethylene and DEE for $Nb_{0.7}$SiBEA testify to greater quantity of acidic sites, on which dehydration reaction occurs. It should be pointed out that only trace amount of DEE was observed in the presence of Nb-free SiBEA zeolite, which may be formed during ethanol etherification on weak Lewis acidic sites [36].

TOF values for NbSiBEA catalysts in the ethanol conversion have been shown in Table 4. Turnover frequency for $Nb_{0.7}$SiBEA is several times higher than for $Nb_{2.0}$SiBEA. Thus, it seems that framework mononuclear Nb(V) efficiently catalyze the processes, which occur on acidic sites (aldol condensation of AA, EtOH dehydration to ethylene and DEE). In addition, TOF of the redox reaction of dehydrogenation for $Nb_{0.7}$SiBEA is almost four times higher than for $Nb_{2.0}$SiBEA, which is consistent with the results obtained for alkenes epoxidation in the presence of aqueous hydrogen peroxide [8].

EtOH/AA mixture conversion. The activity and selectivity of NbSiBEA catalysts were evaluated in the conversion of ethanol and acetaldehyde mixture. Addition of AA (an

intermediate, which takes part in the step of aldol condensation) to EtOH will allow estimating the effect of niobium location in the zeolite matrix on the activity of a catalyst in this step.

In the presence of $Nb_{0.7}SiBEA$ total conversion of EtOH/AA mixture, BD yield (Table 3) and TOF (Table 4) are higher than for $Nb_{2.0}SiBEA$. However, the selectivity to BD is significantly higher for the $Nb_{2.0}SiBEA$ catalyst at 598 K (70.6 %) than for $Nb_{0.7}SiBEA$ (54.8 %) under the same conditions. The selectivity of BD formation at 623 K for both catalysts is close. Decrease in selectivity to BD in the case of $Nb_{2.0}SiBEA$ at higher temperature is attributed to the increase in a rate of thermodynamically more favorable endothermic reaction of EtOH dehydration to ethylene. Change of selectivity to ethylene for $Nb_{2.0}SiBEA$ catalyst from 11.9 % to 29.5 % with increasing of the reaction temperature from 598 to 623 K and selectivity preservation for $Nb_{0.7}SiBEA$ may indicate that dehydration process could occur on LAS, formed by extra-framework Nb(V) species.

Significantly higher TOF values for the dehydration products (ethylene + DEE) is observed on the catalyst, containing only framework mononuclear niobium ($Nb_{0.7}SiBEA$), compared with the sample, containing extra-framework octahedral Nb(V) ($Nb_{2.0}SiBEA$) (Table 4). Thus, it is further evidence of higher activity of framework mononuclear Nb(V), characterized by stronger acidic character than extra-framework octahedral niobium.

It should be noted that higher amount of crotonaldehyde is present in the products of conversion of EtOH/AA mixture on $Nb_{2.0}SiBEA$ (Table 4). The substantial difference in the selectivity to crotonaldehyde, probably, indicates that MPV reduction of crotonaldehyde with EtOH, along with aldol condensation, become key step under the used experimental conditions. Since $Nb_{2.0}SiBEA$ contains less amount of isolated framework mononuclear Nb(V) than $Nb_{0.7}SiBEA$, it can be assumed that MPV reduction of crotonaldehyde proceeds with higher rate in the presence of such niobium species than Nb_2O_5 nanoparticles. A similar conclusion was made for Zr(IV)-based systems [44].

***EtOH/crotonaldehyde mixture conversion*.** Analogous method of intermediate addition was applied in order to estimate the effect of niobium location in the zeolite matrix on the activity of a catalyst in the step of crotonaldehyde MPV reduction to crotyl alcohol. Catalytic performance of the NbSiBEA catalysts in the conversion of EtOH/crotonaldehyde mixture has been shown in Table 5.

The total conversion of EtOH/crotonaldehyde mixture is higher for $Nb_{0.7}SiBEA$ than $Nb_{2.0}SiBEA$. The residual content of crotonaldehyde in the products for both catalysts is low and differs slightly, however, amount of BD as well as ethylene (Table 6) and TOF values (Table 4) are higher for $Nb_{0.7}SiBEA$ than for $Nb_{2.0}SiBEA$. Higher TOF of BD formation than crotonaldehyde reaction, especially for $Nb_{0.7}SiBEA$ catalyst, is a result of conversion of AA, formed in MPV reduction of crotonaldehyde. Thus, the sample containing higher amount of framework mononuclear Nb(V) is more active in the processes, which occur on the surface acidic sites. These results confirm the assumption about the different activity of framework and extra-framework Nb(V) in MPV reduction of crotonaldehyde with EtOH.

3.2.2. Liquid-phase process: synthesis of unsymmetrical ethers

NbSiBEA zeolites with different location of niobium were tested in the liquid-phase tandem process (Scheme 2), including MPV reduction of aldehyde **1** with 2-butanol to 4-methoxybenzyl alcohol (**2**), followed by its etherification with 2-butanol to 4-methoxybenzyl 1-methylpropyl ether (**3**). As well as in the case of ethanol conversion into BD, the catalyst of the process should be bifunctional.

Results of evaluation of catalytic properties of NbSiBEA zeolites in the liquid-phase tandem process are shown on Fig. 11 and Table 6. Higher conversion of aldehyde **1** is observed on the catalyst with greater amount of niobium ($Nb_{2.0}SiBEA$). However, in the presence of the catalyst, containing only framework Nb(V) species ($Nb_{0.7}SiBEA$), aldehyde **1** is completely converted into ether **3**, while on $Nb_{2.0}SiBEA$, containing framework and extra-framework

niobium species, 67 % selectivity to ether **3** is achieved (Table 7). $Nb_{2.0}SiBEA$ is more active in MPV reduction than etherification process as evidenced by higher conversion of aldehyde **1** and incomplete further etherification of alcohol **2**.

Different activity of framework and extra-framework Nb(V) in the etherification was confirmed by the results of the investigation of the reaction of alcohol **2** with 2-butanol in the presence of $Nb_{0.7}SiBEA$ and $Nb_{2.0}SiBEA$ (Table 8). In the presence of $Nb_{0.7}SiBEA$ 93 % conversion of alcohol **2** is achieved after 2 h, while for $Nb_{2.0}SiBEA$ only 37 % is observed after 10 h of the reaction. Moreover, calculated value of TON for $Nb_{0.7}SiBEA$ is significantly higher compared to $Nb_{2.0}SiBEA$. So, we may conclude that specific activity of framework mononuclear Nb(V) is superior than extra-framework octahedral Nb(V).

NbSiBEA catalysts are more active in the etherification and tandem processes in comparison with the zeolites prepared by impregnation of pure silica BEA with ethanolic solutions of Nb(V) ethoxides [14]. Therefore, prepared by two-step postsynthesis method Nb-containing SiBEA zeolite catalysts with framework mononuclear Nb(V) can be alternative materials to hydrothermally synthesized metal-containing zeolites used as catalysts of liquid-phase tandem processes.

4. Conclusions

$Nb_{0.7}SiBEA$ and $Nb_{2.0}SiBEA$ zeolites contain framework mononuclear Nb(V) and mixture of framework mononuclear and extra-framework polynuclear Nb(V), respectively, as evidenced by XRD, NMR, DR UV-vis and FTIR.

The state of niobium in zeolite matrix determines acidic properties and, thus, activity of NbSiBEA catalysts in tandem processes, as was shown for gas-phase and liquid-phase processes.

$Nb_{0.7}SiBEA$ catalyst is more active than $Nb_{2.0}SiBEA$ in the conversion of ethanol and ethanol/acetaldehyde mixture into 1,3-butadiene, MPV reduction of crotonaldehyde with ethanol and etherification of 4-methoxybenzyl alcohol with 2-butanol.

The higher specific catalytic activity (turnover number/frequency) of $Nb_{0.7}SiBEA$ than $Nb_{2.0}SiBEA$ has been revealed for the above mentioned processes.

Thus, two-step postsynthesis preparation procedure allows designing bifunctional NbSiBEA catalysts with redox and acid-base properties required for the occurrence of tandem processes.

Acknowledgements

References

[1]   B. Henrique Arpini, A. de Andrade Bartolomeu, C. Kleber Z. Andrade, L. Carlos da Silva-Filho, V. Lacerda, Curr. Org. Synth. 12 (2015) 570.

[2]   P. Carniti, A. Gervasini, M. Marzo, Catal. Today 152 (2010) 42.

[3]   E.L.S. Ngee, Y. Gao, X. Chen, T.M. Lee, Z. Hu, D. Zhao, Y. Ning, Ind. Eng. Chem. Res. 53 (2014) 14225.

[4]   Z. Xue, Y. Zhang, G. Li, J. Wang, W. Zhao, T. Mu, Catal. Sci. Technol. 6 (2016) 1070.

[5]   K. Subramaniyan, P. Arumugam, J. Porous Mater. 23 (2016) 639.

[6]   X. Gao, I.E. Wachs, M.S. Wong, J.Y. Ying, J. Catal. 203 (2001) 18.

[7]   C. García-Sancho, J.A. Cecilia, A. Moreno-Ruiz, J.M. Mérida-Robles, J. Santamaría-González, R. Moreno-Tost, P. Maireles-Torres, Appl. Catal. B Environ. 179 (2015) 139.

[8]   C. Tiozzo, C. Palumbo, R. Psaro, C. Bisio, F. Carniato, A. Gervasini, P. Carniti, M. Guidotti, Inorganica Chim. Acta 431 (2015) 190.

[9]   A. Gallo, C. Tiozzo, R. Psaro, F. Carniato, M. Guidotti, J. Catal. 298 (2013) 77.

[10]   A. Feliczak-Guzik, A. Wawrzyńczak, I. Nowak, Microporous Mesoporous Mater. 202 (2015) 80.

[11]   O.A. Kholdeeva, Catal. Sci. Technol. 7 (2014) 1869.

[12]   V. V. Ordomskiy, V.L. Sushkevich, I.I. Ivanova, One-Step Method for Butadiene Production, US 8921635 B2, 2014.

[13]   W.J. Toussant, J.T. Dunn, D.R. Jackson, Ind. Eng. Chem. 39 (1947) 120.

[14]   A. Corma, F.X. Llabrés I Xamena, C. Prestipino, M. Renz, S. Valencia, J. Phys. Chem. C 113 (2009) 11306.

[15]   V.L. Sushkevich, D. Palagin, I.I. Ivanova, ACS Catal. 5 (2015) 4833.

[16] P.I. Kyriienko, O. V. Larina, S.O. Soloviev, S.M. Orlyk, S. Dzwigaj, Catal. Commun. 77 (2016) 123.

[17] J. Dijkmans, M. Dusselier, W. Janssens, M. Trekels, A. Vantomme, E. Breynaert, C.E.A. Kirschhock, B.F. Sels, ACS Catal. 6 (2015) 31.

[18] J. Dijkmans, J. Demol, K. Houthoofd, S. Huang, Y. Pontikes, B. Sels, J. Catal. 330 (2015) 545.

[19] S. Dzwigaj, M.J. Peltre, P. Massiani, A. Davidson, M. Che, T. Sen, S. Sivasanker, Chem. Commun. (1998) 87.

[20] S. Dzwigaj, P. Massiani, A. Davidson, M. Che, J. Mol. Catal. A Chem. 155 (2000) 169.

[21] F. Tielens, T. Shishido, S. Dzwigaj, J. Phys. Chem. C 114 (2010) 3140.

[22] S. Dzwigaj, Y. Millot, C. Méthivier, M. Che, Microporous Mesoporous Mater. 130 (2010) 162.

[23] M.A. Camblor, A. Corma, J. Pérez-Pariente, Zeolites 13 (1993) 82.

[24] T. Blasco, M.A. Camblor, A. Corma, P. Esteve, J.M. Guil, A. Martı, S. Valencia, A. Martinez, J.A. Perdigon-Melon, J. Phys. Chem. B 102 (1998) 75.

[25] C.A. Fyfe, H. Strobl, G.T. Kokotailo, C.T. Pasztor, G.E. Barlow, S. Bradley, Zeolites 8 (1988) 132.

[26] G.L. Woolery, L.B. Alemany, R.M. Dessau, A.W. Chester, Zeolites 6 (1986) 14.

[27] L.W. Beck, J.F. Haw, J. Phys. Chem 99 (1995) 1076.

[28] C. Bronnimann, R. Zeigler, G. Maciel, J. Am. Chem. Soc. 110 (1988) 2023.

[29] A. Maciel, G.E.; Ellis, P.D. in: Bell, A.T.; Pines, NMR Techniques in Catalysis, 1994.

[30] M.A. Aramendia, Y. Avil, V. Borau, C. Jim, J.N.L. Marinas, A. Moreno, J.I.L. Ruiz, React. Kinet. Catal. Lett. 65 (1998) 207.

[31]   M. Hartmann, A.M. Prakash, L. Kevan, Catal. Today 78 (2003) 467.

[32]   A.M. Prakash, L. Kevan, J. Am. Chem. Soc. 120 (1998) 13148.

[33]   M. Trejda, A. Tuel, J. Kujawa, B. Kilos, M. Ziolek, Microporous Mesoporous Mater. 110 (2008) 271.

[34]   A. Jentys, N.H. Pham, H. Vinek, J. Chem. Soc. Faraday Trans. 92 (1996) 3287.

[35]   G. Connell, J.A. Dumesic, J. Catal. 105 (1987) 285.

[36]   S. Dzwigaj, N. Popovych, P. Kyriienko, J.-M.J.-M. Krafft, S. Soloviev, Microporous Mesoporous Mater. 182 (2013) 16.

[37]   G. Centi, G. Golinelli, G. Busca, J. Phys. Chem. 94 (1990) 6813.

[38]   T. Hibino, M. Niwa, Y. Murakami, Zeolites 13 (1993) 518.

[39]   A. Corma, V. Fornes, L. Forni, F. Marquez, J. Martınez-Triguero, D. Moscotti, J. Catal. 179 (1998) 451.

[40]   E. V Makshina, M. Dusselier, W. Janssens, J. Degrève, P.A. Jacobs, B.F. Sels, Chem. Soc. Rev. 43 (2014) 7917.

[41]   M. Gao, Z. Liu, M. Zhang, L. Tong, Catal. Letters 144 (2014) 2071.

[42]   C. Angelici, M.E.Z. Velthoen, B.M. Weckhuysen, P.C.A. Bruijnincx, Catal. Sci. Technol. 5 (2015) 2869.

[43]   O. V. Larina, P.I. Kyriienko, S.O. Soloviev, Catal. Letters 145 (2015) 1162.

[44]   V.L. Sushkevich, I.I. Ivanova, E. Taarning, Green Chem. 17 (2015) 2552.

[45]   V.L. Sushkevich, I.I. Ivanova, V. V. Ordomsky, E. Taarning, ChemSusChem (2014) 2527.

[46]   C.A. Emeis, J. Catal. (1993) 347.

Fig. 1. Adsorption isotherms of nitrogen at 77 K for HAlBEA, SiBEA, $Nb_{0.7}$SiBEA and $Nb_{2.0}$SiBEA. For convenience, the dataset for SiBEA, $Nb_{0.7}$SiBEA and $Nb_{2.0}$SiBEA were shifted upwards along the Y-axis.

Fig. 2. XRD patterns of as-prepared HAlBEA, SiBEA, $Nb_{0.7}$SiBEA and $Nb_{2.0}$SiBEA.

Fig. 3. ^{29}Si MAS NMR spectra of as-prepared SiBEA, $Nb_{0.7}$SiBEA and $Nb_{2.0}$SiBEA.

Fig. 4. ^{1}H - ^{29}Si CP MAS NMR spectra of as-prepared SiBEA, $Nb_{0.7}$SiBEA and $Nb_{2.0}$SiBEA.

Fig. 5. ^{1}H MAS NMR spectra as-prepared SiBEA, $Nb_{0.7}$SiBEA and $Nb_{2.0}$SiBEA.

Fig. 6. DR UV–vis spectra of as-prepared $Nb_{0.7}$SiBEA and $Nb_{2.0}$SiBEA.

Fig. 7. FTIR spectra of HABEA, as-prepared SiBEA, $Nb_{0.7}$SiBEA and $Nb_{2.0}$SiBEA, outgassed at 573 K (10^{-3} Pa) for 2 h.

Fig. 8. FTIR spectra of as-prepared SiBEA, $Nb_{0.7}$SiBEA and $Nb_{2.0}$SiBEA.

Fig. 9. FTIR spectra of adsorbed pyridine on $Nb_{0.7}$SiBEA (A) and $Nb_{2.0}$SiBEA (B) catalysts after desorption at different temperatures.

Fig. 10. FTIR spectra of adsorbed 2,6-di-*tert*-butylpyridine on $Nb_{0.7}$SiBEA and $Nb_{2.0}$SiBEA catalysts after desorption at 423 K.

Fig. 11. Synthesis of unsymmetrical ether in the presence of $Nb_{0.7}$SiBEA and $Nb_{2.0}$SiBEA: change of concentrations of 4-methoxybenzaldehyde (1), 4-methoxybenzyl alcohol (2) and 4-methoxybenzyl 1-methylpropyl ether (3). Reaction conditions: aldehyde **1** (1.25 mmol) in 2-butanol (4 g), 100 mg of catalyst, 353 K.

Scheme 1. Overall scheme of ethanol conversion to 1,3-butadiene.

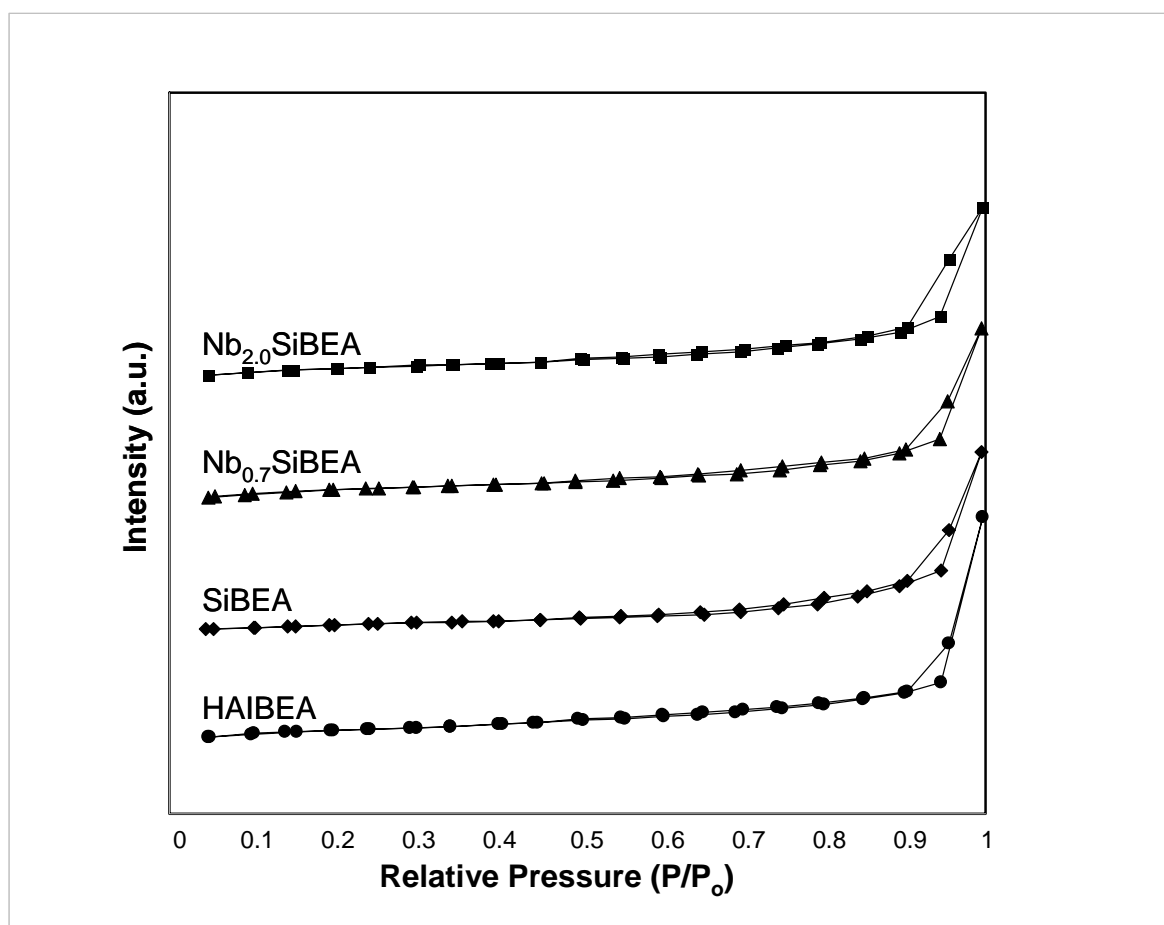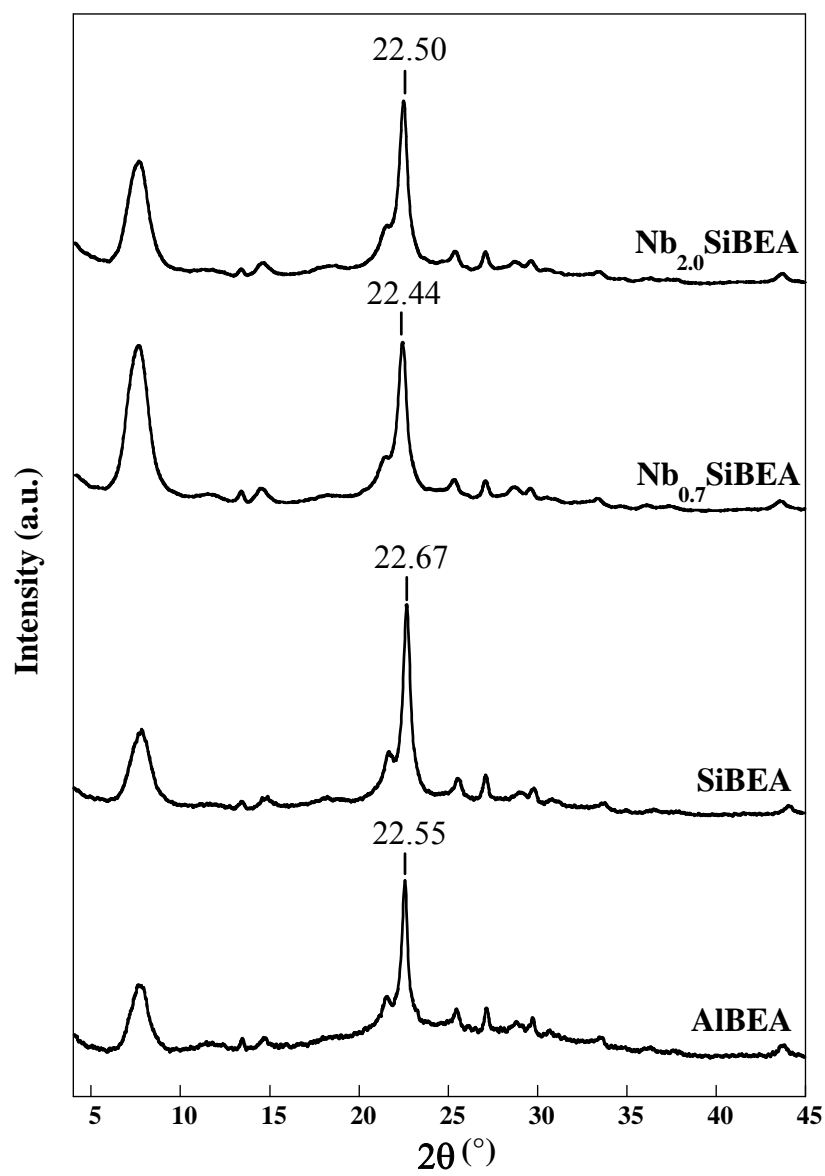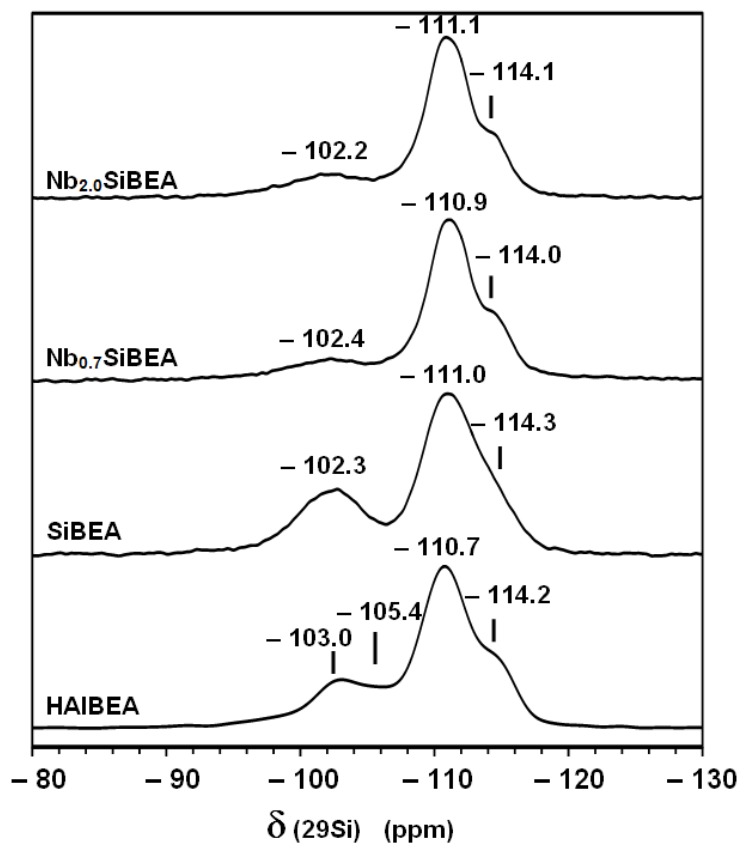**Scheme 2**. Overall scheme of synthesis of unsymmetrical ether.

Fig. 1

Fig. 2.
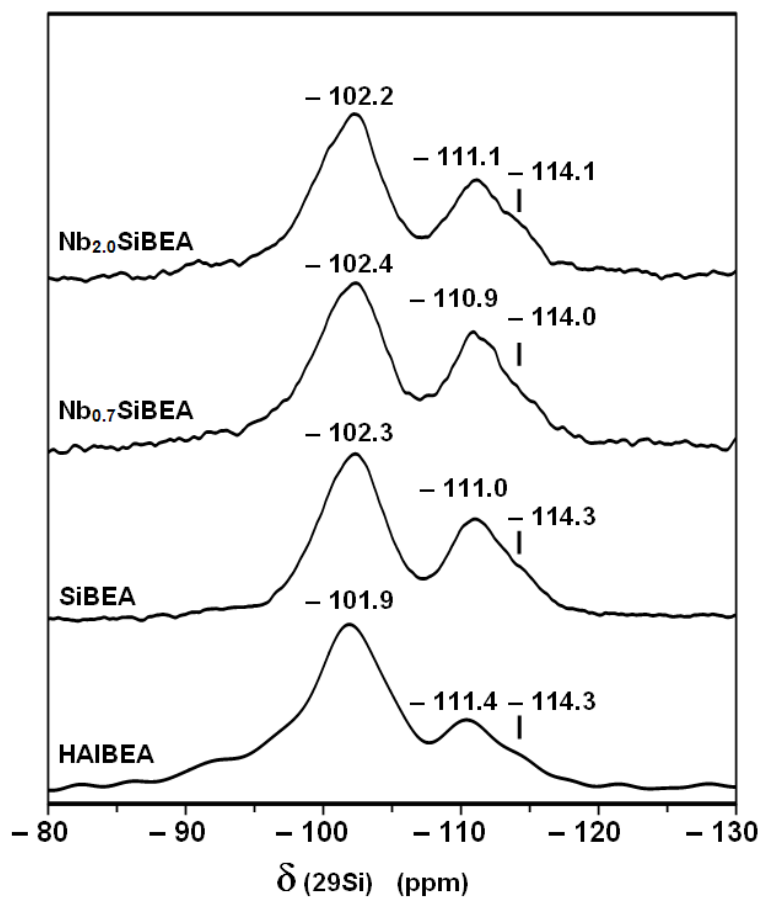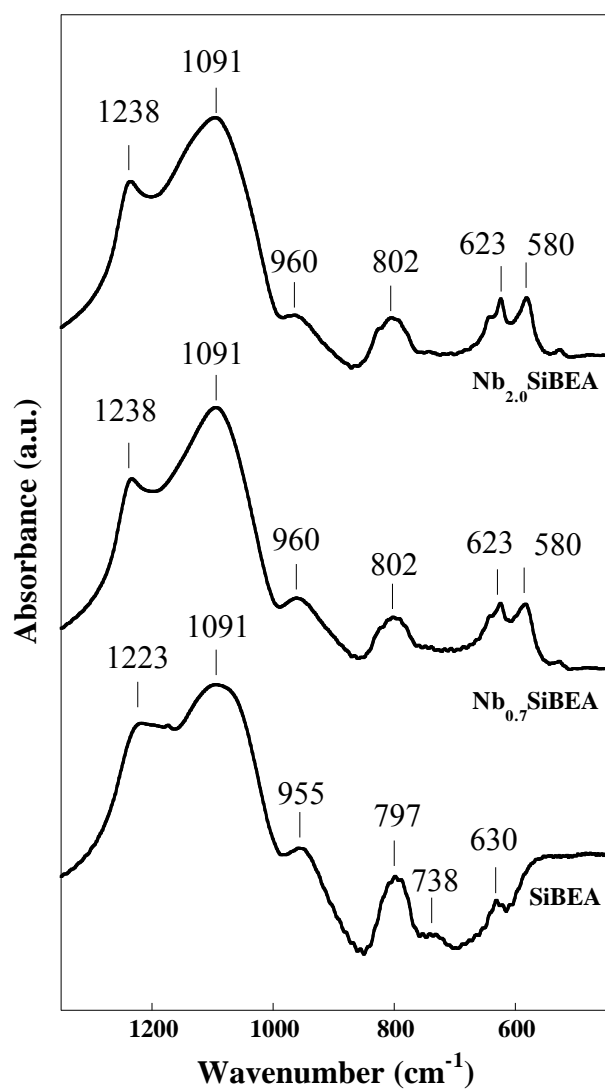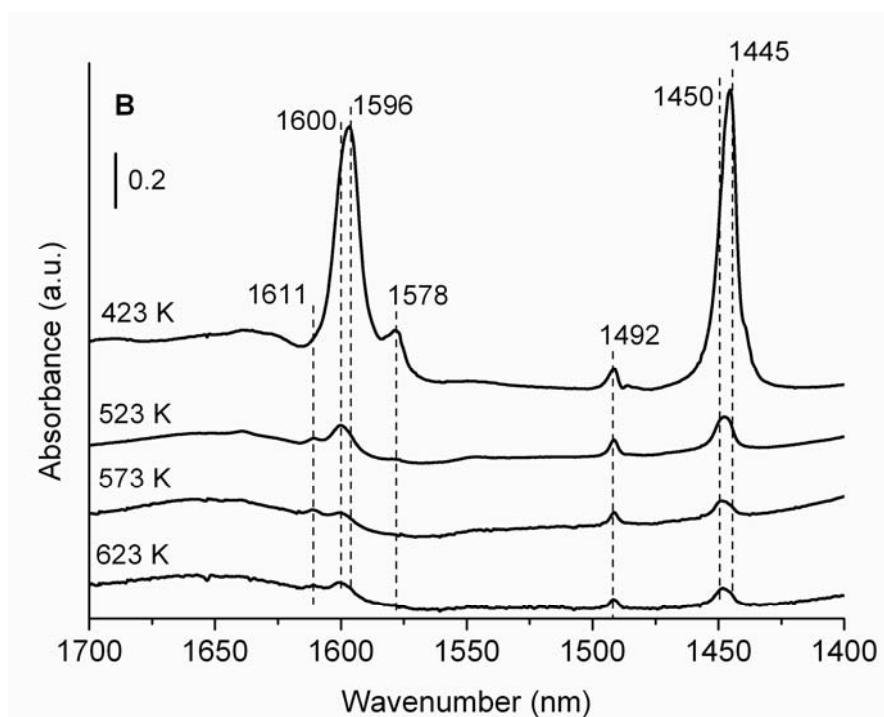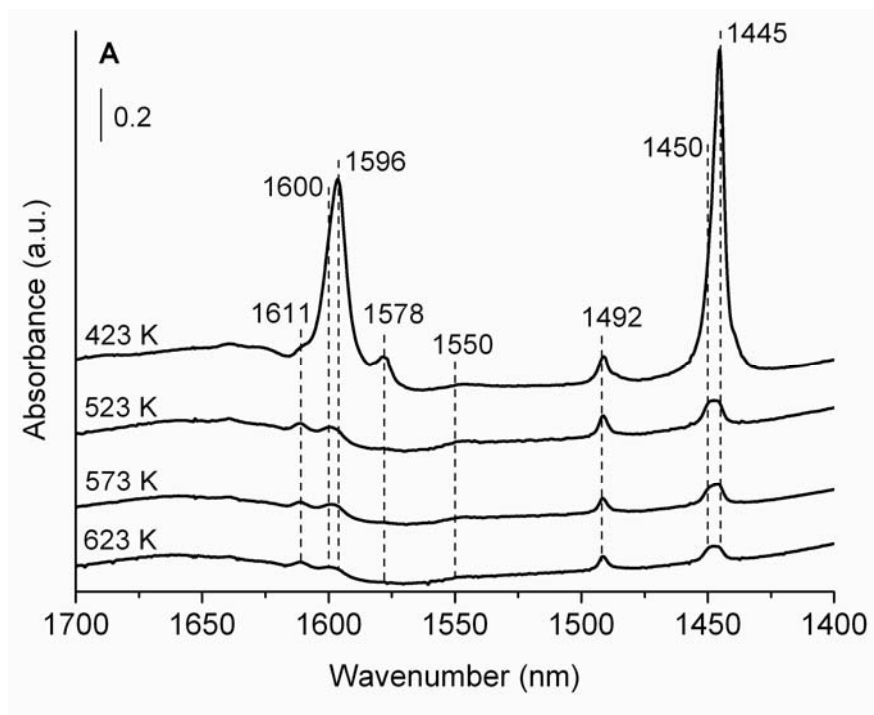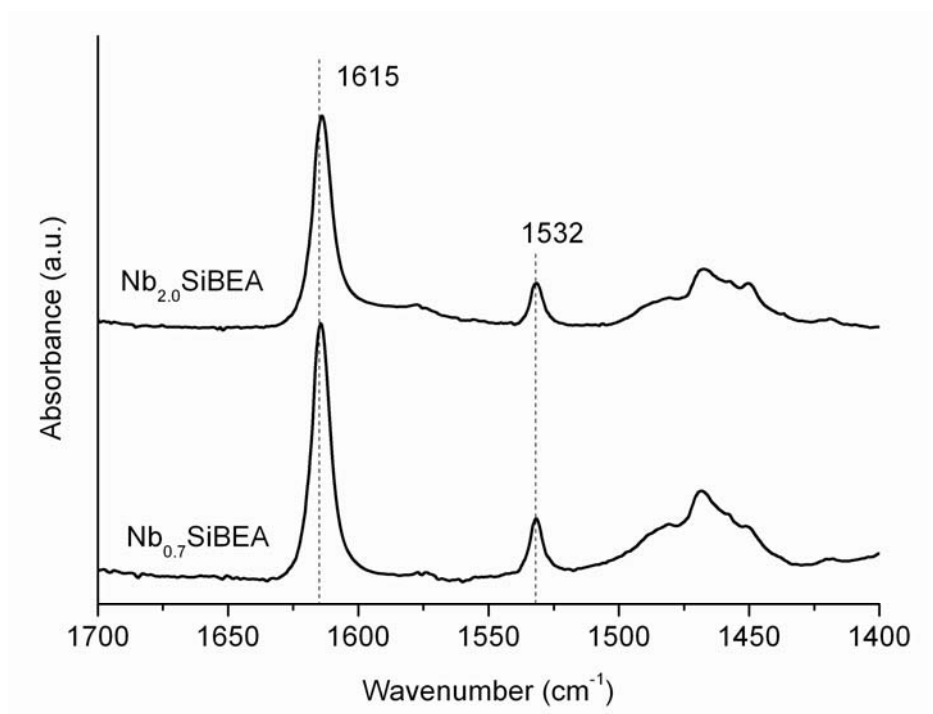
Fig. 3

Fig. 4
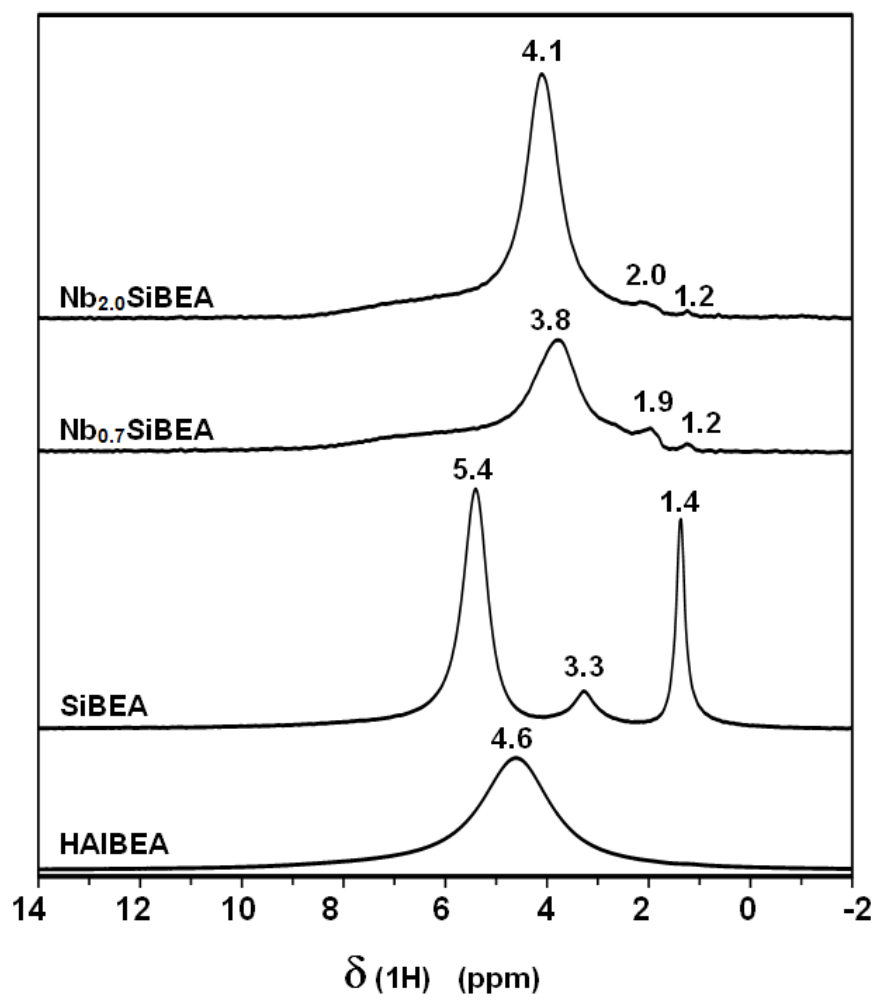
Fig. 5
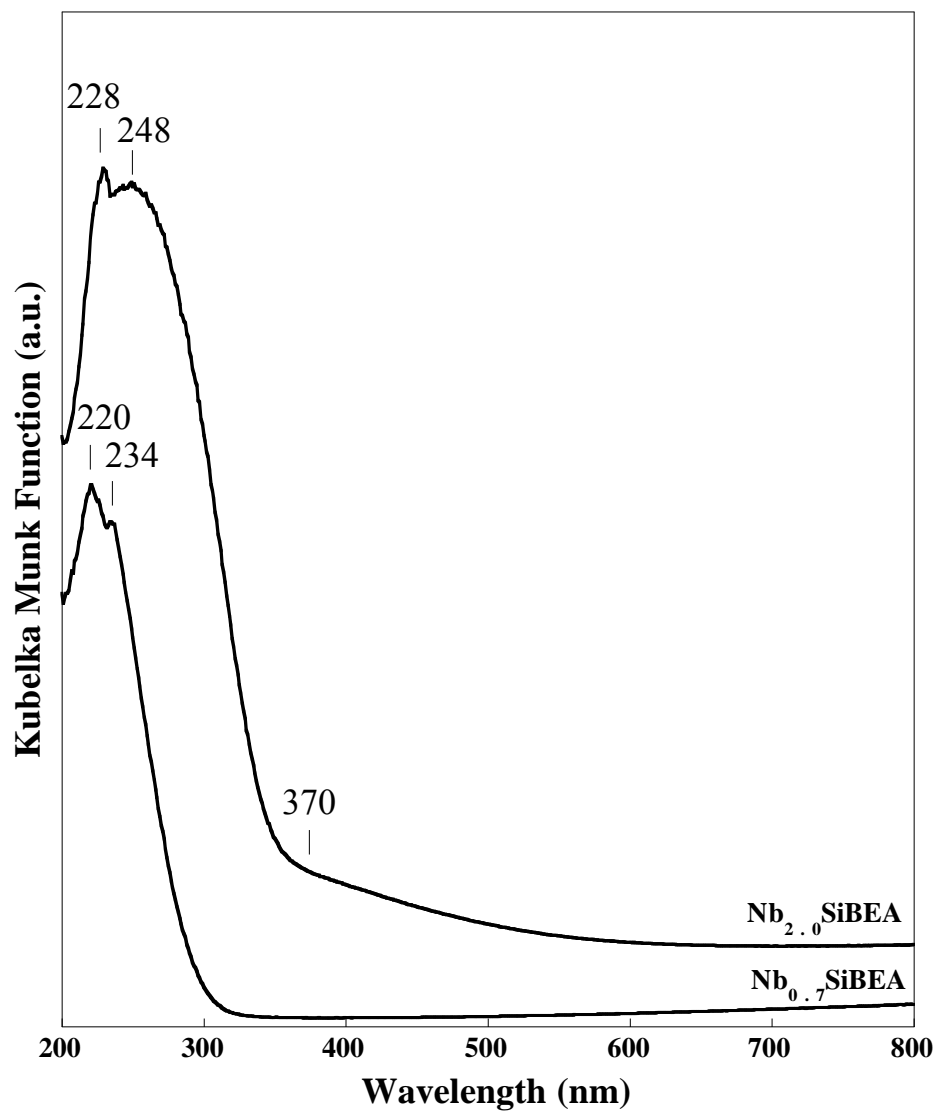
Fig. 6
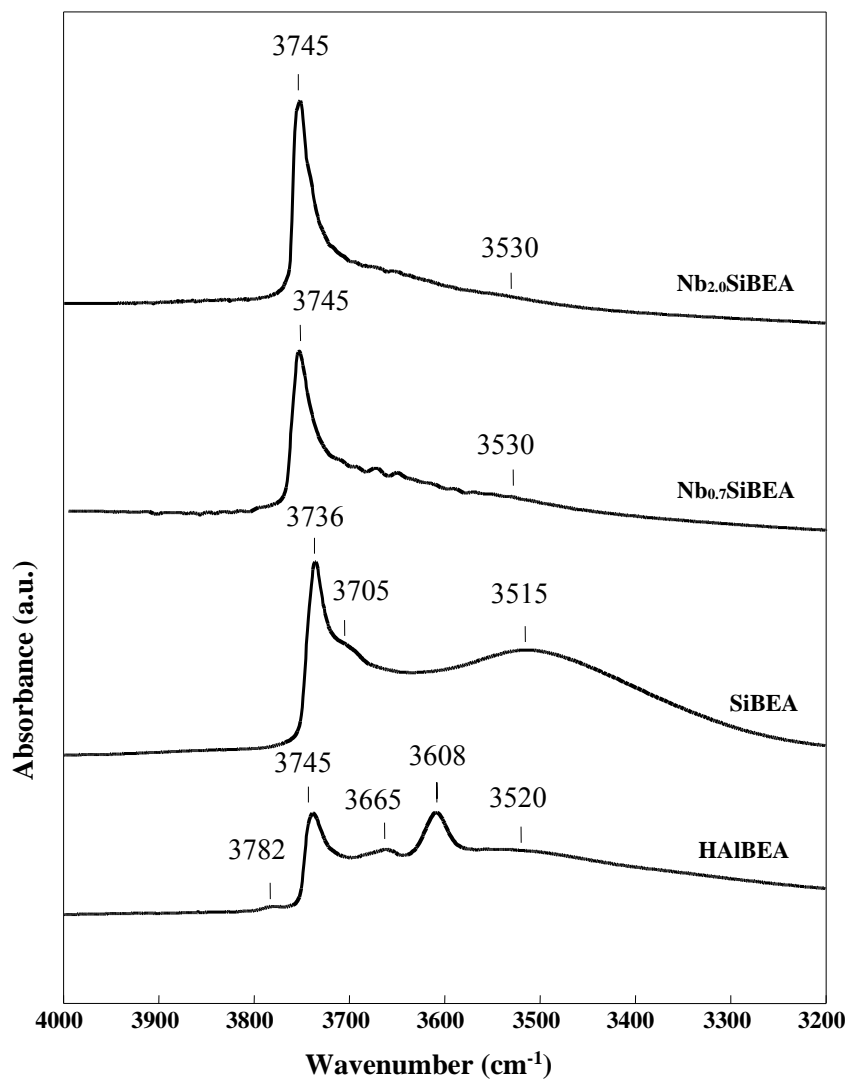
Fig. 7

Fig. 8

Fig. 9

Fig. 10

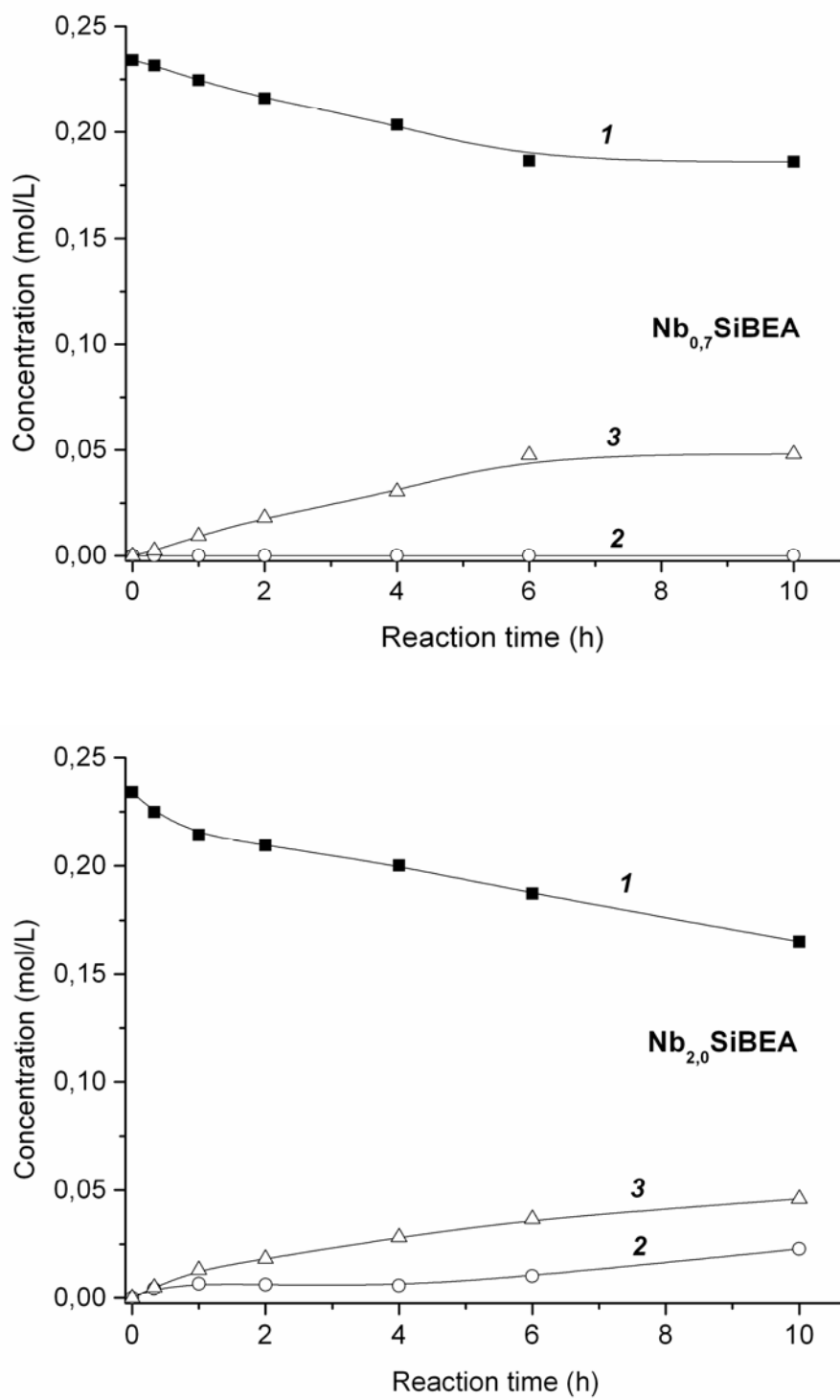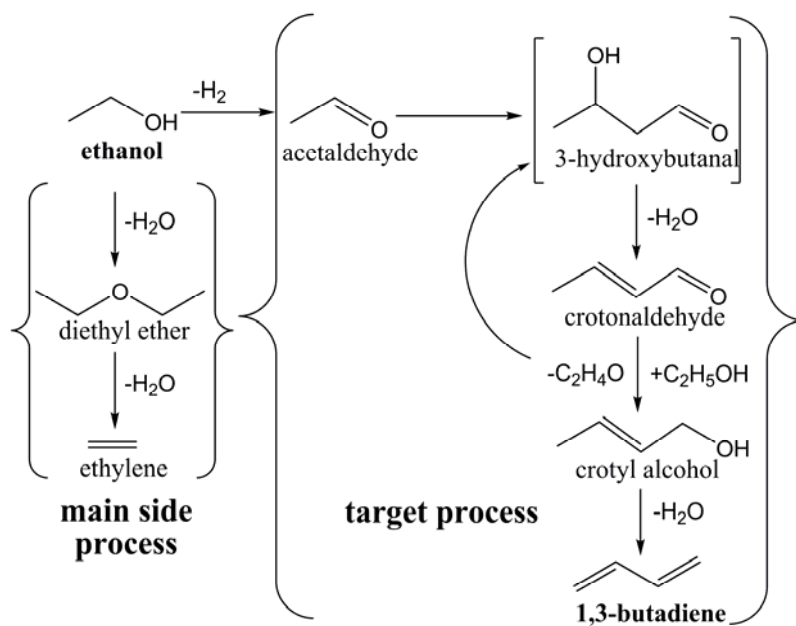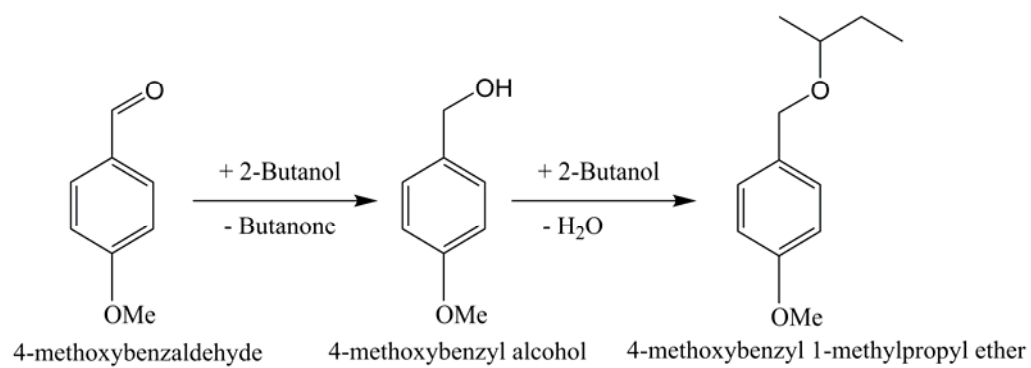**Fig. 11**

Scheme 1.

Scheme 2.

Table 1. Textural properties of zeolite samples.

Sample	Specific surface area, S_{BET} ($m^2\ g^{-1}$)	Micropore volume ($cm^3\ g^{-1}$)
HAlBEA	489	0.20
SiBEA	470	0.19
$Nb_{0.7}SiBEA$	460	0.20
$Nb_{2.0}SiBEA$	491	0.21

Table 2. Concentration of Lewis acidic sites in NbSiBEA[a]

Catalysts	Desorption temperature (K)	Concentration of Lewis acidic sites (mmol·g^{-1})
Nb$_{0.7}$SiBEA	423	40
	523	8
	573	6
	623	4
Nb$_{2.0}$SiBEA	423	51
	523	11
	573	5
	623	4

[a] For a quantitative characterization of LAS, the bands at 1450 cm^{-1} of the FTIR spectra of adsorbed pyridine (Fig. 8) and adsorption coefficient $\varepsilon = 2.22$ μmol·g^{-1} [46] were used.

Table 3. Catalytic performance of the NbSiBEA catalysts in ethanol conversion [a]

T (K)	Total conversion (%)	Product selectivity (C_1 mol%)							BD yield (C_1 mol%)
		BD	AA	ethylene	DEE	butene isomers	croton-aldehyde	others	
Nb$_{0.7}$SiBEA									
598	42.4	27.9	16.8	42.0	12.2	0.5	0.1	0.5	11.9
623	74.6	22.8	11.2	56.9	8.0	0.4	0.1	0.6	17.0
Nb$_{2.0}$SiBEA									
598	27.1	26.0	29.6	28.0	15.6	0.3	0.1	0.4	7.1
623	41.9	19.6	23.5	43.5	12.9	0.2	0.1	0.2	8.2

[a] WHSV = 0.8 $g_{reagents} \cdot g_{cat}^{-1} \cdot h^{-1}$, time-on-stream = 4 h.

Table 4. TOF values for the NbSiBEA catalysts in the gas-phase process at 598 K

Catalyst	TOF (h^{-1})								
	EtOH conversion				EtOH/AA mixture conversion			EtOH/crotonaldehyde mixture conversion	
	EtOH [a]	BD [b]	Ethylene +DEE [b]	Dehydro-genation products [c]	EtOH/ AA [a]	BD [b]	Ethylene +DEE [b]	Croton-aldehyde [a]	BD [b]
Nb$_{0.7}$SiBEA	98	27	53	45	89	49	35	75	111
Nb$_{2.0}$SiBEA	22	6	10	12	18	13	3	26	29

[a] mol of reagent(s) reacted/mol of Nb/hour;

[b] mol of product(s) produced/mol of Nb/hour;

[c] mol of EtOH dehydrogenated to AA, including acetaldehyde, which was converted to C$_4$-products (BD, butene isomers and crotonaldehyde).

Table 5. Catalytic performance of the NbSiBEA catalysts in ethanol/AA mixture conversion [a]

T (K)	Total conversion (%)	Product selectivity (C_1 mol%)						BD yield (C_1 mol%)
		BD	ethylene	DEE	butene isomers	croton-aldehyde	others	
Nb$_{0.7}$SiBEA								
598	38.5	54.8	36.8	2.4	1.2	2.5	2.3	21.1
623	42.8	55.1	36.2	2.3	1.2	3.4	1.8	23.6
Nb$_{2.0}$SiBEA								
598	22.1	70.6	11.9	2.0	1.0	11.8	2.7	15.6
623	25.8	53.1	29.5	3.5	1.1	10.5	2.3	13.7

[a] WHSV = 0.8 $g_{reagents} \cdot g_{cat}^{-1} \cdot h^{-1}$, EtOH/AA=2.7, time-on-stream = 4 h.

Table 6. Catalytic performance of the NbSiBEA catalysts in ethanol/crotonaldehyde mixture conversion [a]

Catalyst	Total conversion (%)	Ratio of components in the stream of the reaction products (C_1 %) [b]							
		BD	AA	ethylene	DEE	butene isomers	croton-aldehyde	EtOH	others
Nb$_{0.7}$SiBEA	85.2	58.2	13.1	8.6	1.3	1.2	1.1	13.7	2.8
Nb$_{2.0}$SiBEA	66.2	43.3	13.5	5.7	1.6	0.8	2.6	31.1	1.4

[a] WHSV = 0.8 $g_{reagents} \cdot g_{cat}^{-1} \cdot h^{-1}$, EtOH/crotonaldehyde = 2, time-on-stream = 2 h;

[b] values are proportional to the yield of a product.

Table 7. Catalytic performance of the NbSiBEA catalysts in 4-methoxybenzaldehyde/2-butanol

conversion [a]

Catalyst	Conversion of aldehyde **1** (%) [b]	Product selectivity (%) [b]		TON
		alcohol **2**	ether **3**	
Nb$_{0.7}$SiBEA	21	0	100	33 [c] / 33 [d]
Nb$_{2.0}$SiBEA	29	33	67	16 [c] / 11 [d]

[a] Reaction conditions: aldehyde **1** (1.25 mmol) in 2-butanol (4 g), 100 mg of catalyst, 353 K;

[b] after 10 h;

[c] mol of reacted aldehyde **1**/mol of Nb;

[d] mol of aldehyde **1** converted to ether **3**/mol of Nb.

Table 8. Catalytic performance of the NbSiBEA catalysts in 4-methoxybenzyl alcohol/2-butanol etherification [a]

Catalyst	Conversion of alcohol **2** (%)			TON [b]
	2 h	4 h	10 h	
Nb$_{0.7}$SiBEA	93	99	100	292
Nb$_{2.0}$SiBEA	18	24	37	21

[a] Reaction conditions: alcohol **2** (2.5 mmol) in 2-butanol (4 g), 100 mg of catalyst, 353 K;

[b] mol of reacted alcohol **2**/mol of Nb.